Induction of glycosylation in human C-reactive protein under different pathological conditions

Tanusree DAS*, Asish SEN*, Tore KEMPF†, Sumit R. PRAMANIK*, Chhabinath MANDAL‡ and Chitra MANDAL*[1]

*Immunobiology Division, Indian Institute of Chemical Biology, 4 Raja S.C. Mullick Road, Calcutta 700 032, India, †Protein Analysis Facility, German Cancer Research Center, INF280, 69120 Heidelberg, Germany, and ‡Drug Design, Development and Molecular Modelling Divisions, Indian Institute of Chemical Biology, 4 Raja S.C. Mullick Road, Calcutta 700 032, India

As an acute-phase protein, human C-reactive protein (CRP) is clinically important. CRPs were purified from several samples in six different pathological conditions, where their levels ranged from 22 to 342 μg/ml. Small, but significant, variations in electrophoretic mobilities on native PAGE suggested differences in molecular mass, charge and/or shape. Following separation by SDS/PAGE, they showed single subunits with some differences in their molecular masses ranging between 27 and 30.5 kDa, but for a particular disease, the mobility was the same for CRPs purified from multiple individuals or pooled sera. Isoelectric focusing (IEF) also indicated that the purified CRPs differed from each other. Glycosylation was demonstrated in these purified CRPs by Digoxigenin kits, neuraminidase treatment and binding with lectins. The presence of N-linked sugar moiety was confirmed by N-glycosidase F digestion. The presence of sialic acid, glucose, galactose and mannose has been demonstrated by gas liquid chromatography, mass spectroscopic and fluorimetric analysis. Matrix-assisted laser-desorption ionization analysis of the tryptic digests of three CRPs showed systematic absence of two peptide fragments, one at the N-terminus and the other near the C-terminus. Model-building suggested that the loss of these fragments exposed two potential glycosylation sites on a cleft floor keeping the protein–protein interactions in pentraxins and calcium-dependent phosphorylcholine-binding qualitatively unaffected. Thus we have convincingly demonstrated that human CRP is glycosylated in some pathological conditions.

Key words: acute-phase protein, glycosylation, lectin binding, matrix-assisted laser-desorption ionization analysis (MALDI analysis), molecular modelling.

INTRODUCTION

C-reactive protein (CRP) is the first reported acute-phase protein in humans ([1] and references therein). It belongs to a highly conserved phylogenetically ancient family called pentraxins, which have five identical non-covalently linked subunits ([2] and references therein). At the present time, there are no reports suggesting that human CRP is glycosylated. CRPs are characterized by their calcium-dependent ligand-binding affinity for the phosphorylcholine (PC) moiety of pneumococcal C-polysaccharide [1,3]. In spite of the *in vitro* demonstration of the involvement of CRPs in a variety of biological events, their precise physiological role is yet to be established. In humans, the CRP level is low (0.1–0.5 μg/ml) under normal conditions, but increases up to approx. 1000-fold during inflammation [1], making CRP probably the single most useful molecule for monitoring acute-phase reactions.

CRP has diverse roles in the host defence mechanism [4–6]. It binds to chromatin, histones, small nuclear ribonucleoprotein particles and galactose-containing polysaccharides [1,4,5]. Increased synthesis of CRP is triggered by certain cytokines including interleukin-6, interleukin-1, growth factor β, and some other extracellular signalling molecules [3,7,8].

The relationship between the structural aspects of CRP in various disease states has not yet been investigated. To the best of our knowledge, there are no reports on comparative studies of the molecular nature of human CRP in various diseases. Are the induced proteins similar or different? Does any correlation exist between CRPs purified from diverse clinical samples at the molecular level? If so, do structural differences exist amongst these CRP molecules? Do these differences have an impact on their biological functions? Answers to these questions may well provide a better insight into their mechanism of action. Unfortunately, at present, in general, human CRP levels are used only as a non-specific diagnostic marker. It may be envisaged that the structure–function relationship of human CRP modified differently in different clinical conditions can serve as a biochemical model for studying acute-phase reactions.

In earlier reports, we demonstrated the induction of different molecular variants of CRP under different toxic aquatic conditions in freshwater fish, which was due to differences in amino-acid and carbohydrate compositions [5,9–12]. The main aim of the present investigation is the identification, purification and characterization of CRPs from six different pathological conditions, thereby establishing that human CRP is glycosylated.

To the best of our knowledge, this is the first report of the induction of novel glycosylation in human CRP. Based on the sequence data, computer-aided molecular modelling revealed two potential sites for glycosylation on the cleft floor, which opens up due to slight changes in the sequence without affecting other functional areas of the pentraxin structures. Our results provide a new structural insight into the unique glycosylated molecular variants of CRP induced in different clinical conditions.

Abbreviations used: ALL, acute lymphoblastic leukaemia; BSTFA, bis(trimethylsilyl)trifluoroacetamide; ConA, concanavalin A; CRP, C-reactive protein; DIG, digoxigenin; IEF, isoelectric focusing; MAA, *Maackia amurensis* agglutinin; MALDI, matrix-assisted laser-desorption ionization; NC, nitrocellulose; PC, phosphorylcholine; RCA, *Ricinis communis* agglutinin; SLE, systemic lupus erythematosus; SNA, *Sambucus nigra* agglutinin; TMCS, trimethyl chlorosialane; VL, visceral leishmaniasis.

[1] To whom correspondence should be addressed (e-mail cmandal@iicb.res.in or Chitra_mandal@yahoo.com).

Table 1 Status of CRPs in seven different clinical samples

Serial no.	Clinical samples*	CRP in crude sample†	Purified CRP (μg/ml)‡	Fold increase§	Presence of carbohydrate‖
1	Systemic lupus erythematosus (SLE)	++	342.0	684	1+
2	Acute lymphoblastic leukemia (ALL)	+++	21.3	42	2+
3	Tuberculosis	+++	78.0	156	3+
4	Visceral leishmaniasis (VL)	+++	24.0	48	3+
5	Cushing's syndrome	+++	75.3	150	1+
6	Osteogenic sarcoma (pleural fluid)	+++	33.0	66	2+
7	Osteogenic sarcoma (serum)	++	71.2	142	–

* CRPs were purified from serum of all clinical samples except osteogenic sarcoma, where serum and pleural fluid were used.

† Polystyrene latex particles coated with anti-CRP antibodies were used; reactivity of CRP present in crude sample was graded as medium (++) and strong (+++) depending on the degree of visible agglutination.

‡ Purified CRP was estimated by using a known molar absorption coefficient.

§ Fold increase was calculated compared with 0.5 μg/ml as the normal level.

‖ As determined using the DIG glycan detection kit. The extent of glycosylation as reflected in the intensity of the spots are graded by '+' numbers; '–' represents absence of carbohydrate in CRP.

MATERIALS AND METHODS

Reagents

Sepharose CL4B was from Amersham Biosciences, Agarose was from Bio-Rad, and *p*-nitrophenyl PC and PC chloride were from Sigma. The PC affinity matrix was prepared as previously described in [9]. The Rhelax-CRP kit was from The Tulip Group (Mumbai, India), and the Digoxigenin (DIG) glycan detection kit, the DIG glycan differentiation kit and the deglycosylation kit were from Boehringer Mannheim. Bis(trimethylsilyl)-trifluoroacetamide (BSTFA) and trimethyl chlorosialane (TMCS) were from Pierce, Rockford, IL, U.S.A. All other chemicals were of analytical grade.

Study population and design

Samples were collected from patients with acute and chronic infections and other disorders (Table 1). The samples were sent to the Indian Institute of Chemical Biology, Calcutta, India, where they were screened individually for detectable levels of CRP by latex agglutination by using the Rhelax-CRP kit. Samples that showed detectable agglutination were included in this study. Informed consent was obtained from all individuals and the study was carried out in accordance with the Institutional Human Ethical Clearance Committee.

Purification of human CRP

CRPs from each individual sample were separately purified to apparent homogeneity, taken either from sera or pleural fluid of patients, and also from pooled sera of several individuals suffering from the same disease, following a standard protocol as described by Volanakis et al. [13]. Typically, human serum (approx. 4 ml) from a patient was passed through a column of agarose beads (1 cm × 5 cm) in the presence of Tris-buffered saline (TBS; 50 mM Tris/HCl and 150 mM NaCl), pH 7.5, with $CaCl_2$ (5 mM) to remove the serum amyloid-P component. This serum, free of the serum amyloid-P component, was immediately applied to Sepharose–PC (1 cm × 10 cm) affinity matrix, washed with TBS (20 mM Tris/HCl) and $CaCl_2$ (10 mM), pH 7.5 and bound protein was eluted with EDTA (10 mM) containing $CaCl_2$ (1 mM). Protein fractions were pooled, dialysed against TBS (20 mM Tris/HCl), before adjusting the calcium concentration to 10 mM, and were allowed again to bind to another Sepharose–PC affinity matrix. The column was washed with TBS containing $CaCl_2$ (10 mM) and pure CRP was eluted with PC (2 mM) in TBS (20 mM Tris/HCl), pH 7.5, containing $CaCl_2$ (0.5 mM). The eluted protein was extensively dialysed against Hepes (0.02 M) with saline containing EDTA (2 mM), followed by washing with the same buffer without EDTA, and storage at −20 °C. Protein content was estimated using the molar absorption coefficient at 280 nm of 19.50.

PAGE

CRPs purified from patients with six different pathological conditions were analysed by native (5, 7.5 and 10% gel) and SDS/PAGE (7.5–15% gradient gel) under both reducing and non-reducing conditions [14,15]. Gels were stained with silver nitrate. Molecular masses of the subunits were determined by using standard SDS/PAGE markers along with purified human IgG. As assayed by immunoblotting of the gel using polyclonal anti-human IgG antiserum, the preparation of purified CRP contained no detectable amounts of IgG confirming its purity.

ELISA

In addition, an ELISA was performed to detect any possible contamination of human IgG with the CRP sample. Equal amounts of purified CRP and human IgG were coated separately on to the polystyrene surface of a 96-well plate and were washed with 20 mM phosphate buffer, 150 mM NaCl and 1% (v/v) Tween 20. Horseradish peroxidase-tagged anti-(human IgG) was added after blocking non-specific, followed by detection with substrate. When CRP was allowed to bind with anti-(human IgG), negligible absorbance was observed in comparison with when an equal amount of pure IgG was coated on to the plate in parallel, confirming the absence of detectable IgG contamination in CRP preparation.

IEF

Analytical IEF [16] of affinity-purified CRPs (1.5 μg) was carried out in capillary tubes on an ampholine polyacrylamide gel (4%), pH range 3.5–10.0, using the Mini-PROTEAN II tube cell apparatus (Bio-Rad). The samples were focused at a constant voltage of 400 V for 6 h. The focused tube gels were fixed, washed and stained with silver nitrate. The pI of each individual protein was determined as a function of its migration from the cathode using standard proteins (Sigma). CRP was desialylated by neuraminidase from *Arthrobacter ureafaciens* (0.5–1 m-units)

in 75 mM sodium acetate buffer, pH 5.5, at 37 °C overnight and analysed by IEF.

Detection of carbohydrate

Total sugars present in purified CRPs were qualitatively detected using the DIG-glycan detection kit. In brief, hydroxyl groups of sugar residues were oxidized with metaperiodate to yield aldehyde. Oxidized CRPs were either spotted on to nitrocellulose (NC) or separated by SDS/PAGE, followed by transfer on to NC. DIG bound to aldehyde was detected by enzyme-conjugated anti-DIG antibodies and was visualized by appropriate substrate.

Total sialic acids were measured fluorimetrically using pure sialic acid as a standard [17]. In brief, purified CRPs were oxidized by sodium metaperiodate and processed before and after saponification of the O-acetyl group. The relative fluorescence intensity ($\lambda_{max(exitation=410\ nm)}/\lambda_{max(emision=510\ nm)}$) of each sample was measured against the reagent blanks on a Hitachi F-4010 spectrofluorimeter (Tokyo, Japan). The percentage of (8)9-O-acetylated sialic acid was determined by subtracting the respective unsubstituted sialic acids from that obtained after de-O-acetylation.

The presence of sialic acid was analysed using the DIG glycan differentiation kit. Two commercially available plant lectins namely, *Sambucus nigra* agglutinin (SNA) and *Maackia amurensis* agglutinin (MAA) were used.

Determination of carbohydrate composition by GLC and GLC–MS

Neutral sugars present in purified CRPs were detected by GLC as their alditol acetates [18]. The samples (50–100 μg) were hydrolysed with 2 M trifluoroacetic acid at 120 °C for 90 min in a sealed glass tube to liberate monosaccharides, followed by reduction with sodium borohydride (10 mg). Resulting alditols were acetylated with distilled pyridine and acetic anhydride [1 ml; 1:1 (v/v)] at room temperature (25 °C) for 16 h. Alditol acetates were analysed by GLC and GLC–MS. The constituent sugars were identified from the retention time of authentic sugars and/or from their mass fragmentation pattern in electron impact (EI) mode. GLC was performed using a Hewlett-Packard 6890 plus gas chromatograph equipped with a flame ionization detector. For the detection and quantification of the peaks, a Hewlett-Packard 3380A chemstation was used. For resolution, a fused silica capillary column HP-5 (30 m, 0.32 mm, 0.25 μm) and nitrogen as carrier gas were used with a temperature programme of 150 °C (5 min), 2 °C (1 min) and 200 °C (10 min) at split less mode. For GLC–MS [19], a Hewlett-Packard gas chromatograph 5890 series II tandemly linked to a Jeol mass spectrometer (JEOL AX-500) with electron impact ionization at 70 ev and ion source temperature at 200 °C was used. HP-5 MS (25 m, 0.25 mm, 0.25 μm) using a temperature programme of 160 °C (7 min), 2 °C (1 min) and 210 °C (5 min) with helium as carrier gas and in split less mode was used for analysis.

Analysis of sialic acids by GLC

CRPs (100 μg) were hydrolysed with 0.1 M trifluoroacetic acid at 80 °C for 1 h to release the sialic acid. The hydrolysates were evaporated at reduced pressure. Traces of acid were removed by co-distillation three times with 0.5 ml water. The samples in reactive vials were dried under vacuum over P_2O_5 for 4 h and were dissolved in 10 μl of anhydrous pyridine. The BSTFA with 1 % TMCS (10 μl) was added to each vial under nitrogen and was allowed to react for 2 h at room temperature. Samples were then analysed by GLC using a fused silica HP-5 column (30 m, 0.32 mm, 0.25 μm) at 210 °C isothermal conditions. The peaks were compared with that of standard silyl derivative of N-acetylated neuraminic acid.

Lectin-binding assay

CRPs were iodinated with $Na^{125}I$ using the chloramine T method [20]. ^{125}I-labelled CRPs were incubated separately (at fixed concentrations) with 20 μl of Sepharose/agarose-bound lectins of different sugar linkage and specificity, e.g. concanavalin A (ConA), wheat germ agglutinin (WGA), *Dolichus biflorus* agglutinin (DBA), *Ricinus communis* agglutinin (RCA), *Helix pomatia* agglutinin (HPA), *Limulus polyphemus* agglutinin (LPA), *Ulex europaeus* agglutinin (UEA) overnight at 4 °C. After extensive washing to remove non-specific binding, bound CRPs were monitored in a γ-counter. All experiments were performed in triplicates.

Detailed analysis of ConA binding

Iodinated CRP with increasing concentrations was incubated with a fixed amount of ConA–Sepharose (20 μl) in TBS (20 mM), pH 7.2, containing Ca^{2+}, Mg^{2+} and Mn^{2+} (1 mM each) at 4 °C overnight. Counts were taken after washing to remove non-specific binding, and bound radioactivity was measured by a γ-counter and was plotted against the concentration of CRP. The apparent association constant was calculated from the Scatchard plot [21,22] in which bound/free was plotted against varying amounts of bound CRP. The experiment was repeated with CRPs purified from different clinical samples.

To confirm the specificity of the ConA–CRP binding, different concentrations of mannose (0–400 mM) were added separately to pre-equilibrated reaction mixtures containing a fixed amount of iodinated CRP and ConA–Sepharose (20 μl). After overnight incubation at 4 °C and washing, radioactivity was monitored. An unrelated sugar, e.g. galactose, was also included in this study.

Deglycosylation of CRPs for SDS/PAGE analysis

To reconfirm the presence of sugars in the induced CRPs, they were deglycosylated using the deglycosylation kit. Briefly, fixed amounts of CRPs purified from six different clinical samples were incubated overnight with *Arthrobacter ureafaciens* neuraminidase (specific activity, 0.5 m-unit) in denaturation buffer [100 mM sodium phosphate, 10 mM EDTA, 0.5 % (w/v) Triton X-100, 0.05 % (w/v) SDS and 1 % (v/v) 2-mercaptoethanol] at pH 8.6 at 37 °C. The reaction mixture was heated at 100 °C for 3 min, centrifuged, before the addition of reaction buffer [20 mM sodium phosphate, 10 mM EDTA, 0.5 % (v/v) Nonidet P40, 0.5 % (w/v) CHAPS and 0.05 % (w/v) SDS], pH 7.2, and N-glycosidase F were added and the mixture was incubated overnight at 37 °C. In the case of O-glycosidase (1–2 m-units) or a combination of N and O glycosidase treatment, neuraminidase-treated samples were incubated overnight with the enzymes in potassium phosphate buffer containing EDTA, Triton X and SDS, pH 7.3 at 37 °C. Deglycosylated CRPs were analysed by SDS/PAGE.

Matrix-assisted laser-desorption ionization (MALDI) MS

Coomassie Blue-stained protein bands were excised from the gel, repeatedly washed with water and water/acetonitrile and finally shrunk with acetonitrile. Proteins were digested in the

gel with trypsin (sequencing grade modified porcine trypsin from Promega) in 40 mM ammonium bicarbonate overnight at 37 °C. The peptides generated in the supernatant were analysed by MALDI MS. Sample preparation was achieved following the thin film preparation techniques [23]. Briefly, 0.3 μl aliquots of a NC-containing saturated solution of α-cyano-4-hydroxycinnamic acid in acetone were deposited on to individual spots on the target. Subsequently, 0.8 μl of 10 % formic acid and 0.4 μl of the digested sample was loaded on top of the thin film spots and allowed to dry at ambient temperature. To remove salts from the digestion buffer, the spots were washed with 10 % formic acid and with water.

MALDI mass spectra were recorded in the positive ion mode with delayed extraction on a Reflex II time-of-flight instrument (Bruker-Daltonik GmbH, Bremen, Germany) equipped with a SCOUT multiprobe inlet and a 337 nm nitrogen laser. The ion acceleration voltage was set at 20.0 kV, the reflector voltage was set at 21.5 kV and the first extraction plate was set at 15.5 kV. Mass spectra were obtained by averaging 50–200 individual laser shots. Calibration of spectra was performed internally by a two-point linear fit using the autolysis products of trypsin at *m/z* 842.50 and 2211.10.

Protein modelling and structural analysis

Molecular modelling was carried out based on the reported structure of human CRP [2]. Models of modified CRP were constructed from the X-ray crystallographically determined structures of human CRP (1GNH) and its complex with Ca^{2+} and PC (1B09) using knowledge-based homology modelling using InsightII 98.0 (Accelrys, San Diego, CA), ABGEN [24] and our in-house package of MODELYN and ANALYN (version PC-1.0, 1998; developed by C. Mandal) in the Unix environment. Energy minimization and molecular dynamics were performed with the InsightII 98.0/Discover package using cff 91 force field on a Silicon Graphics® OCTANE workstation. Energy minimizations were performed with a convergence criterion of 4.184 J/mol (0.001 kcal/mol), using a combination of steepest descent and conjugate gradient methods (100 steps each). The structure of the segment of the modified CRP was regularized by repeated steps of molecular dynamics (100 steps of equilibration and 1000 steps of dynamics with a conformation sampling after every ten steps, followed by the selection of the minimum energy conformation) and energy minimization (100 steps each of descent and conjugate gradient) until satisfactory conformational parameters were obtained.

RESULTS

Affinity purification of human CRPs

CRPs were purified separately either from individual patients or from pooled sera of a few individuals suffering from systemic lupus erythematosus (SLE), acute lymphoblastic leukaemia (ALL), tuberculosis, visceral leishmaniasis (VL), Cushing's syndrome, osteogenic sarcoma. CRP was also purified from pleural fluid of an individual suffering from osteogenic sarcoma. Pure protein eluted as a single peak from the affinity column and also showed a single peak in HPLC. The induced CRP levels varied significantly from 22–342 μg/ml of serum (Table 1), corresponded to a 42–684-fold increase above the normal level (0.5 μg/ml), confirming that CRP was an acute-phase reactant in these pathological conditions.

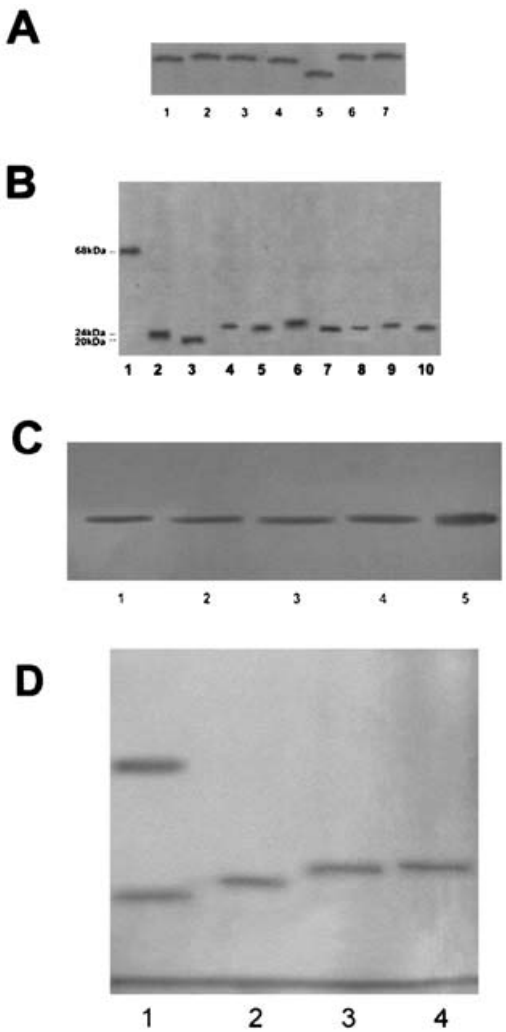

Figure 1 Analysis of CRPs by gel electrophoresis

(**A**) Affinity-purified CRPs (1 μg) were analysed by native PAGE (5 % gel), as described in the Materials and methods section, and the gel was silver stained. Lanes 1–5 represent CRPs from the sera of SLE, ALL, tuberculosis, VL and Cushing's syndrome respectively. CRPs from the pleural fluid and the serum of a patient suffering from osteogenic sarcoma are shown in lanes 6 and 7. (**B**). CRPs (1 μg) were separated by gradient SDS/PAGE (7.5–15 %). The molecular mass standards BSA (68 kDa), trypsinogen (24 kDa) and trypsin inhibitor (20 kDa) were run (lanes 1–3) along with equal amounts of CRP purified from sera of SLE, ALL, tuberculosis, VL, Cushing's syndrome and osteogenic sarcoma (pleural fluid and serum) respectively (lanes 4–10). (**C**) Equal amount of CRPs (1 μg/well), purified from four different individuals suffering from VL, were analysed by SDS/PAGE (lanes 1–4). Lane 5 contained a mixture of equal amounts (380 ng of each) of CRPs pooled from all four individuals. (**D**) An equal amount of purified human IgG (lane 1), along with three CRPs (2 μg/well), purified from ALL (serum), osteogenic sarcoma (pleural fluid) and Cushing's syndrome (serum) (lanes 2, 3 and 4) were analysed by SDS/PAGE.

Differences in electrophoretic mobilities

Figure 1(A) shows the native gel (5 %) electrophoretic patterns of purified CRPs from SLE, ALL, tuberculosis, VL, Cushing's syndrome (lanes 1–5) and osteogenic sarcoma (both from pleural fluid and serum, lanes 6 and 7) showing a single band confirming their electrophoretic homogeneity. The samples demonstrated small differences from each other in their mobilities, while CRP from Cushing's syndrome (lane 5) showed markedly different mobility, suggesting differences in molecular mass, charge and/or structure. Similar patterns were also observed when analysed on 7.5 and 10 % native gels. With SDS/PAGE (Figure 1B), each

purified CRP gave a single subunit both under reducing and non-reducing conditions. The molecular mass of subunits varied from 27–30.5 kDa (lanes 4–10).

Purified CRPs from several individuals of each group suffering from the SLE, ALL, tuberculosis, VL, Cushing's syndrome and osteogenic sarcoma were analysed by SDS/PAGE. Interestingly, it was found that each sample from a particular group gave a single band and moved to the same position indicating identical subunits. A representative profile of CRP from four individual VL patients is presented in Figure 1(C), lanes 1–4. They also moved to an identical location when mixed together in equal amounts before electrophoresis (Figure 1C, lane 5). Alternatively, CRP purified from the pooled sera of five individual patients suffering from SLE showed a single band, indicating that the same subunit is present in the CRP of all five individuals. Similar results were also obtained for sets of five individual patients suffering from ALL, tuberculosis, VL, Cushing's syndrome and osteogenic sarcoma.

Figure 1(D) shows SDS/PAGE patterns of pure human IgG (lane 1) along with three CRPs (lanes 2, 3 and 4), purified from ALL (serum), osteogenic sarcoma (pleural fluid) and Cushing's syndrome (serum) respectively. No heavy chain of IgG corresponding to approx. 50 kDa in lanes 2, 3 and 4 was detected even on silver staining. Single bands of 27, 29 and 30 kDa corresponding to the subunits of three CRPs were observed. This profile clearly shows the absence of human IgG even in trace amounts.

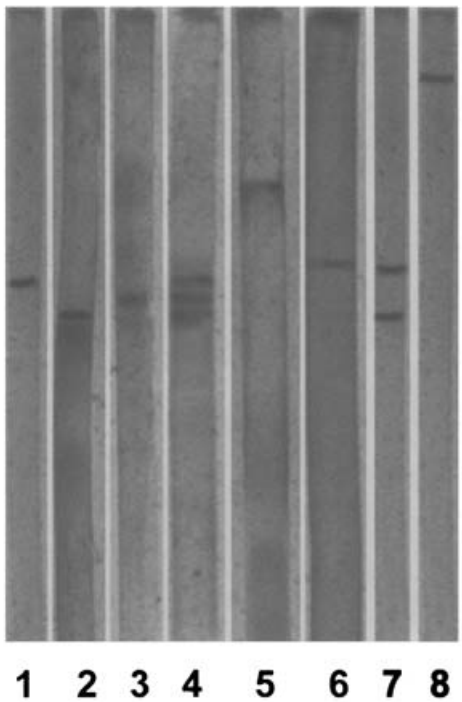

Figure 2 IEF of CRPs

Purified CRP (1.5 μg) was applied to an ampholine polyacrylamide tube gel (4 %) in a pH gradient (3.5–10) as described in the Materials and methods section. The gel was stained with silver nitrate. Representative profiles of CRPs purified from ALL, Cushing's syndrome, SLE, a mixture of these three CRPs (1.5 μg of each CRP), CRPs from tuberculosis and osteogenic sarcoma (pleural fluid) are shown in lanes 1–6 respectively. CRP from sera of VL patients before and after neuraminidase treatment are shown in lanes 7 and 8.

IEF

To investigate the charge heterogeneity, affinity-purified CRPs were run on an IEF gel. In general, CRP showed a single band (Figure 2), confirming their purity and the presence of a single molecular entity. However, CRPs from sera of ALL, Cushing's syndrome, SLE, tuberculosis and pleural fluid of osteogenic sarcoma (lanes 1–3, 5 and 6) showed slight differences in their pI values (8.1, 7.9, 8.0, 9 and 8.7 respectively). A mixture of three CRPs purified from three clinical samples (ALL, Cushing's syndrome and SLE) is shown in lane 4. It is noteworthy that they segregated to three distinct bands and moved to their respective positions, suggesting the presence of three different molecular variants. However, CRP from a VL patient showed more than one band, of pI 7.9 and 8.6 (lane 7), using IEF despite showing only a single band following SDS/PAGE. Interestingly, neuraminidase treatment of the same sample resulted in a single band with an increase in pI to 10.0 (lane 8), demonstrating the presence of sialic acid.

Detection of sugars by the DIG glycan detection kit

The presence of sugars was demonstrated in CRP samples using the DIG glycan detection kit by dot blot (Figure 3A). Columns 1–7 represent seven CRPs purified from seven clinical samples from SLE, ALL, tuberculosis, VL, Cushing's syndrome and osteogenic sarcoma (from pleural fluid and serum). Columns 8 and 9 containing fetuin and buffer served as positive and negative controls respectively. All the clinical samples (columns 1–6) were glycosylated except for CRP purified from the serum of a patient suffering from osteogenic sarcoma (column 7). This non-glycosylated CRP was used as a control in many experiments. Interestingly, CRP from pleural fluid of the same patient showed completely different reactivity; in pleura, it was glycosylated (column 6), whereas in serum, it was not (column 7). More importantly, the variable amount of glycosylation was reflected in the intensities of the spots that differed prominently from each other (Table 1; Figure 3A). The presence of sugar on the individual band of CRP was also demonstrated after Western blot on NC paper (Figure 3B).

Quantitative estimation of sialic acids

In view of the differential mobility in native PAGE and IEF, the possibility of the variation of negatively charged sugars, sialic acid and its commonest derivative, namely (8)9-O-acetylated sialic acid, was examined by quantitative fluorimetric analysis. Results from six different clinical samples revealed the presence of these derivatives in purified human CRPs (Table 2) confirming again the glycosylation of CRP. Differences in the sialic acid content (5.1–13.5 ng/μg of CRP) and (8)9-O-acetylated sialic acid (3.8–23 % of total sialic acid) probably contributes towards the variability observed in CRP induced in these pathological conditions. Interestingly, sialic acid could not be detected in non-glycosylated CRP (which served as control).

Differential occurrence of linkage-specific sialic acid epitopes

The variable expression of linkage-specific sialic acids was demonstrated using a DIG glycan differentiation kit (Figure 3C). A representative dot blot of CRPs purified from pleural fluid and serum of patients with osteogenic sarcoma (column 1) and Cushing's syndrome (column 2), respectively, showed the differential reactivities with two sialic-acid-binding lectins SNA and MAA, which are known to recognize α2–6 and α2–3

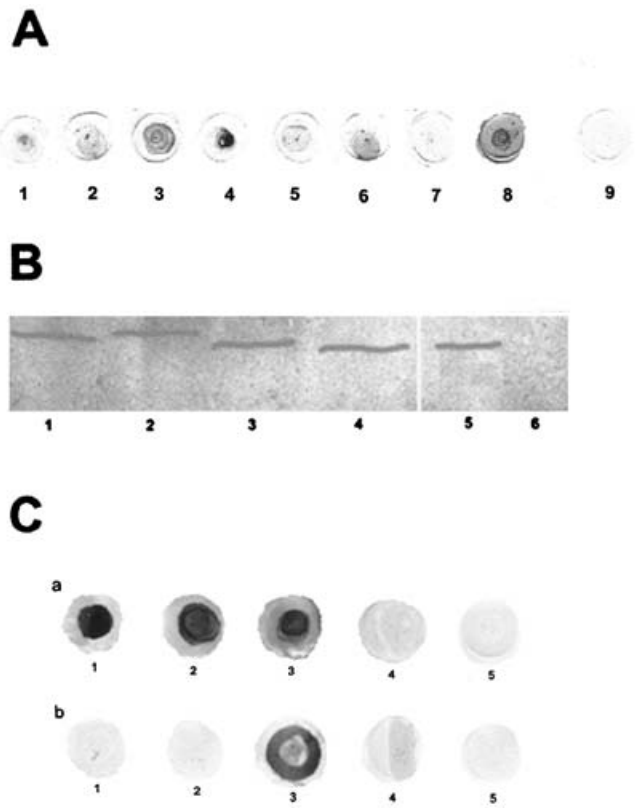

Figure 3 Detection of sugars in CRPs by an enzyme immunoassay using a DIG glycan kit

(**A**) DIG glycan detection by the dot blot method. Purified CRPs (1.0 μg) were blotted on to NC strips and were processed for detection of neutral sugar using a DIG kit. Columns 1–6 represent six CRPs purified from sera of SLE, ALL, tuberculosis, VL, Cushing's syndrome and pleural fluid of osteogenic sarcoma respectively. Non-glycosylated CRP purified from serum of a patient with osteogenic sarcoma is shown in column 7. Columns 8 and 9 represent positive and negative controls respectively. (**B**) DIG glycan detection after SDS/PAGE and Western blot analysis. Purified CRPs (2.0 μg) were oxidized with metaperiodate, separated by SDS/PAGE, transferred on to nitrocellulose and were processed for detection of the aldehyde group using a DIG kit. Lanes 1–4 represent CRPs from VL, tuberculosis, SLE and ALL respectively. Lanes 5 and 6 are positive and negative controls respectively. (**C**) Detection of sialic acids by a DIG glycan differentiation kit. Columns 1 and 2 of panels a and b represent the reactivity of two CRPs purified from pleural fluid of osteogenic sarcoma and serum of Cushing's syndrome with SNA and MAA respectively. Columns 3 and 4 of both panels are the corresponding positive and negative controls respectively. Column 5 of both panels represents a non-glycosylated CRP purified from the serum of an osteogenic sarcoma patient. Panels a and b were blotted with SNA and MAA respectively as described in the Materials and methods section.

sialylgalactosyl residues respectively. Interestingly, MAA showed no binding (Figure 3C, panel b, columns 1 and 2), whereas strong reactivity was observed with SNA in both CRPs (Figure 3C, panel a, columns 1 and 2). High amounts of SNA-specific sialoglycans were found on these two CRPs indicating the predominance of α2-6-linked sialic acids in these molecules, conclusively indicating that CRP is glycosylated. On the other hand, non-glycosylated CRP purified from the serum of a patient suffering from osteogenic sarcoma showed no reactivity with SNA and MAA (Figure 3C, column 5, panels a and b).

Variation in carbohydrate composition by GLC and GLC–MS

In order to search for the origin of the observed heterogeneity of different CRPs in PAGE analysis, the carbohydrate compositions were determined by GLC and GLC–MS. A representative profile of the analysis of CRP purified from the serum of a patient suffering from tuberculosis is presented in Figure 4(A). The GLC chromatogram peaks revealed the presence of three hexoses, namely mannose, glucose and galactose. A representative profile of mass fragmentation of the CRP purified from a patient showed several inter alia peaks, having *m/z* values of 361, 289, 259, 217, 187, 170, 145, 127, 128, 115, 103, 97, which confirmed further the presence of hexitol hexa-acetates (Figure 4B). The sialic acid content of all three CRPs was also determined by GLC. A representative profile of CRP purified from an ALL patient is shown in Figure 4(C). The GLC chromatogram peaks revealed the presence of sialic acid as compared with the standard silyl derivative of *N*-acetylneuraminic acid. Non-glycosylated CRP was used as a control. No detectable peak was observed.

Table 2 Fluorimetric quantitation of sialic acid and (8)9-O-acetylated sialic acid

Purified CRPs (1.0 μg) were oxidized by sodium metaperiodate before and after saponification of the O-acetyl group and were processed as described in [17]. Pure sialic acid was used as standard. The percentage of (8)9-O-acetylated sialic acid was determined by subtracting the relative unsubstituted sialic acid from that obtained after de-O-acetylation.

Clinical samples	Total sialic acid (ng/μg of CRP)	(8)9-O-acetylated sialic acid (% of total sialic acid)
SLE	6.8	11.0
ALL	13.5	20.0
Tuberculosis	7.0	14.0
VL	12.0	16.8
Cushing's syndrome	8.5	3.8
Osteogenic sarcoma (pleural fluid)	5.1	23.0
Osteogenic sarcoma (serum)	Not detected	

Table 3 Binding of CRPs with lectins of varying specificity

For this experiment, CRPs were iodinated and the labelled proteins were incubated separately (at a fixed concentration) with Sepharose/agarose-bound lectins (20 μl) of different sugar specificity and linkage, e.g. ConA, wheat germ agglutinin (WGA), *Dolichus biflorus* agglutinin (DBA), RCA, *Helix pomatia* agglutinin (HPA), *Limulus polyphemus* agglutinin (LPA), *Ulex europaeus* agglutinin (UEA), overnight at 4 °C. After washing to remove any non-specific adhered lectins, bound CRPs were monitored in a γ-counter.

			Binding (%)			
		CRP...	Osteogenic sarcoma	SLE	VL	ALL
Lectin	Sugar and linkage specificity	Source...	Pleural fluid	Serum	Serum	Serum
ConA	α-Man, α-Glc		13.0	4.8	6.7	6.5
WGA	GlcNAc, Neu5Ac		11.8	6.5	2.4	3.7
DBA	α-GalNAc		18.8	6.1	1.9	2.7
RCA	β-D-Gal (GalNAc, β-Gal)		29.2	8.8	5.7	7.0
HPA	α-or β-D-GalNAc		16.0	6.4	3.1	2.7
LPA	Neu5Ac		1.9	0.7	2.2	2.4
UEA	α-L-Fuc		12.3	5.6	3.1	1.4

CRPs are glycosylated as demonstrated by ConA binding

Glycosylation of CRP was demonstrated further by the binding of CRPs with ConA, a non-glycosylated mannose-binding lectin. Quantitatively, the binding of CRPs to ConA showed variations (Table 3). Among the four different CRPs presented here, CRP purified from the pleural fluid of osteogenic sarcoma patients showed the highest binding (13.0%) indicating the presence of more glucose and mannose. In contrast, the binding was only 6.7, 6.5 and 4.8% with CRPs purified from VL, ALL

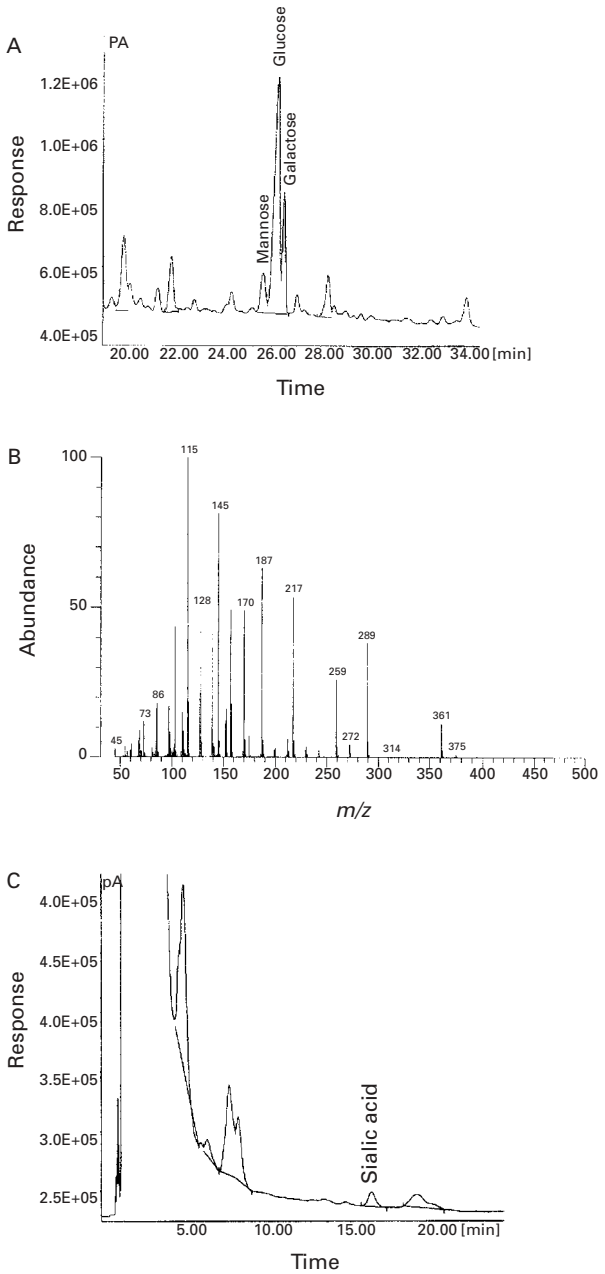

Figure 4 Analysis of carbohydrate composition by GLC and GLC-MS

A representative profile for the presence of three hexoses in purified CRP (100 μg) from a tuberculosis patient as analysed by GLC. The analysis was carried out as described in the Materials and methods section. Response (in picoamperes, pA) was plotted against time (in min). The individual peaks reveal the presence of glucose, galactose and mannose (**A**). The sample was also analysed by GLC–MS and shown as a plot of abundance against *m/z* (**B**). A representative profile for the presence of sialic acid in CRP (100 μg) purified from an ALL patient as analysed by GLC as a trimethylsilyl derivative (**C**). The peak was compared with that of standard silyl derivative of *N*-acetylneuraminic acid. Response (in picoamperes, pA) was plotted against time (in min).

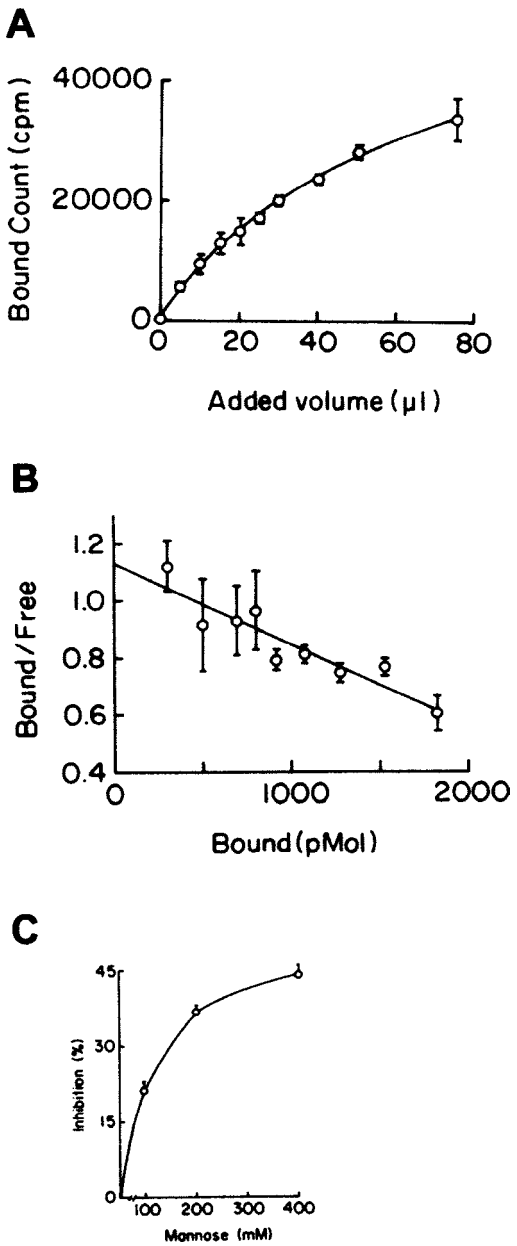

Figure 5 Scatchard analysis and specificity of CRP binding with ConA

A fixed amount of ConA–Sepharose (20 μl/tube) was incubated with various concentrations of iodinated CRP (specific radioactivity 5.4×10^8 c.p.m./mg) purified from an ALL patient. Bound radioactivity at different titration points are plotted against the volume (μl) of CRP added (**A**). The apparent association constant was obtained from the Scatchard plot (**B**) in which bound/free was plotted against various amounts of bound CRP (pmol). (**C**) Replacement of CRP from the Con A–CRP complex with mannose. ConA–Sepharose (20 μl) was allowed to bind with a fixed concentration of CRP (10 μl, 1.3×10^4 c.p.m.) purified from a VL patient in ConA buffer as described in the Material and methods section. The binding of ConA–CRP was replaced by incubating the reaction mixture with mannose (0–400 mM). The radioactivity of bound CRP was measured before and after incubation with mannose and the extent of inhibition (%) was plotted as a function of mannose concentration (mM).

and SLE respectively. Binding constants were determined for the binding of ConA with four different CRPs. The binding of a fixed amount of ConA with different amounts of iodinated CRP purified from an ALL patient is presented in Figure 5(A) and the corresponding Scatchard plot is shown in Figure 5(B). Apparent binding constants (K_a) of CRPs purified from sera of SLE, ALL and VL, and pleural fluid of osteogenic sarcoma were 2.03×10^8, 2.84×10^8, 0.61×10^8 and 3.08×10^8 M^{-1}, with the corresponding dissociation constants being 4.93, 3.52, 16.4 and 3.25 nM respectively as calculated by Scatchard analysis.

Mannose inhibits ConA binding with CRP

To examine the binding specificity, the binding of CRP to ConA was measured at increasing concentrations of mannose

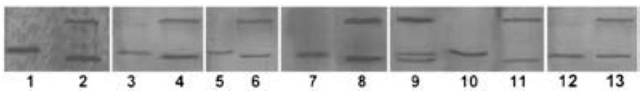

Figure 6 SDS/PAGE analysis of N-glycosidase F-digested CRP

A representative profile of glycosylated CRPs purified from five individuals suffering from osteogenic sarcoma, ALL, VL, tuberculosis and SLE as analysed by SDS/PAGE is shown in lanes 1, 3, 5, 8 and 10 respectively. An aliquot of each sample was digested separately with N-glycosidase F (10 units) at 37 °C overnight and analysed similarly (lanes 2, 4, 6, 7 and 11 respectively). A mixture of undigested and digested CRP purified from an SLE patient is shown in lane 9. The upper band in each enzyme-treated lane corresponds to N-glycosidase F (34.6 kDa). Protein bands were detected by silver staining. Non-glycosylated CRP purified from the serum of an osteogenic sarcoma patient (used as a control) is shown in lanes 12 and 13 before and after digestion with enzyme.

(0–400 mM; Figure 5C). Bound CRP from VL patient was replaced only at higher concentrations of mannose (about 44 % at 400 mM), indicating high lectin specificity towards the mannose/glucose moiety present in CRP. A high concentration of mannose may be due to a stronger affinity of ConA for sugar linkages present in CRP than for a simple sugar. This experiment clearly demonstrates the presence of mannose/glucose residues, again confirming that the CRP is glycosylated. A similar concentration of galactose could not inhibit this binding.

Decrease in molecular mass of deglycosylated CRP in SDS/PAGE

A representative gel showing the mobility of glycosylated CRPs purified from pleural fluid of osteogenic sarcoma, and sera of ALL, VL, tuberculosis and SLE, before and after N-glycosidase F digestion, is presented in Figure 6. It may be noted that there is a decrease in the molecular mass of 2–4 kDa after enzyme treatment. A mixture of undigested and digested CRP purified from SLE (lane 9) showed a decrease of 4 kDa after deglycosylation. Non-glycosylated CRP, even after enzyme treatment, moved to the same location (lanes 12 and 13). The upper band in each enzyme-treated lane corresponds to N-glycosidase F (34.6 kDa). On the other hand, no change in the electrophoretic mobility was observed following O-glycosidase digestion of the same samples, once again reaffirming that CRP is glycosylated possibly through N-linkage.

Variations in lectin-binding properties

Structural differences in the carbohydrate moieties of these molecular variants of CRP were demonstrated further in their differential binding properties towards the seven different lectins tested. A wide variation was observed in the lectin binding properties of CRP from four different pathological conditions (Table 3). It may be noted that CRP from pleural fluid of osteogenic sarcoma showed higher binding towards all lectins in general, compared with other CRPs. The extent of binding was highest with RCA, being 5.3-, 4.1- and 3.3-fold more compared with other CRPs purified from VL, ALL and SLE patients respectively.

MALDI analysis

In addition to variation in glycosylation, amino-acid sequences of different CRP samples underwent MALDI analysis of the tryptic fragments obtained from the CRPs purified from three patients. The peptide masses matching tryptic fragments were mapped on to the sequence (underlined in Figure 7). Table 4 presents

```
1           11          21          31          41
MEKLLCFLVL TSLSHAFQQT DMSRKAFVFP KESDTSYVSL KAPLTKPLKA
51          61          71          81          91
FTVCLHFYTE LSSTRGYSIF SYATKRQDNE ILIFWSKDIG YSFTVGGSEI
101         111         121         131         141
LFEVPEVTVA PVHICTSWES ASGIVEFWVD GKPRVRKSLK KGYTVGAEAS
151         161         171         181         191
IILGQEQDSF GGNFEGSQSL VGDIGNVNMW DFVLSPDEIN TIYLGGPFSP
201         211         221
NVLNWRALKY EVQGEVFTKP QLWP
```

Figure 7 N- and C-terminal sequence analysis

Purified CRP samples were examined by MALDI analysis [32,33]. Coomassie Blue-stained protein bands were digested with trypsin and the peptides generated were analysed. Sample preparation was achieved following the thin film preparation techniques. MALDI mass spectra were recorded in the positive ion mode with delayed extraction. Mass spectra were obtained by averaging 50–200 individual laser shots. Calibration of spectra was performed internally by a two-point linear fit using the autolysis products of trypsin at *m/z* 842.50 and 2211.10. The peptide masses matching with tryptic fragments were mapped on to the sequence (underlined) of human CRP. The amino acids are represented using one-letter codes.

Table 4 Sequence analysis

Coomassie Blue-stained protein bands were excised from the gel, washed and digested in the gel with trypsin overnight at 37 °C. The peptides generated in the supernatant were analysed by MALDI MS [23]. Sample preparation was achieved following the thin film preparation techniques as described in the Material and methods section. MALDI mass spectra were recorded in the positive ion mode with delayed extraction. Mass spectra were obtained by averaging 50–200 individual laser shots. Calibration of spectra was performed internally by a two-point linear fit using the autolysis products of trypsin at *m/z* 842.50 and 2211.10.

	Missing peptide fragments in purified CRP	
Patient	N-terminal amino acids (1–6) QTDMSR	C-terminal amino acids (189–191) ALK
Osteogenic sarcoma	–	–
ALL	–	+
Cushing's syndrome	–	–

the tryptic fragments obtained from MALDI analysis of three CRP samples isolated from patients with osteogenic sarcoma, Cushing's syndrome and ALL. Examination of these fragments indicates the systematic absence of two peptide fragments, one N-terminal fragment of six amino acids (QTDMSR; first bold segment in Figure 7) after the leader sequence in all the samples and another fragment near the C-terminus of three amino acids (ALK; second bold segment in Figure 7) from CRPs of patients with osteogenic sarcoma and Cushing's syndrome. The leader sequence of the first 18 amino acids was not present in any of the three CRP preparations tested, which is expected for a matured CRP.

Molecular modelling

Molecular modelling was carried out to examine the effect of absence of the specific fragments on the structure of human CRP. Analysis of the model of the modified CRP shows that the structural motifs containing all the prominent known functions of human CRP remained very nearly unaffected. In Figure 8(A), the native pentraxin structure is shown with the missing segments (in the modified CRP) coloured light pink and white; it is evident that these motifs are away from the monomer–monomer interface of the pentraxin. The same result was also obtained from the calculation of the inter-atomic distances, since none of the affected atoms were within the 4 Å; (1 Å = 0.1 nm) of the interface, except for the tail of the side chain of the Arg^{6} in subunit A in the AB interface of the pentraxin. The Ca^{2+}- and PC-binding

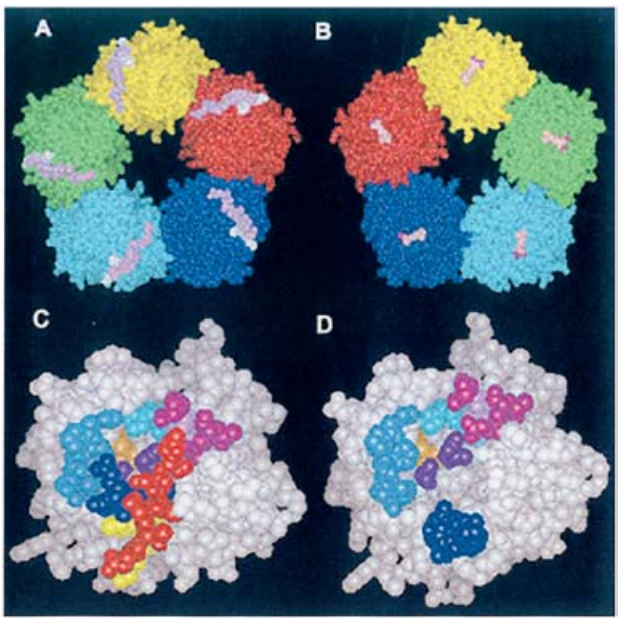

Figure 8 Molecular modelling

(**A**), (**B**) Pentraxin structure of CRP. (**A**) shows the pentraxin structure of human CRP taken from 1B09. Structural motifs absent in the CRP extracted from diseased samples are marked with light pink (amino acids 1–6, QTDMSR) and white (amino acids 189–191, ALK). (**B**) shows the back view (180 ° rotation along the X-axis) of the structure, which exposes calcium (coloured light pink) and PC (coloured deep pink) bound to the CRP. (**C**), (**D**) Single subunit of CRP. (**C**) shows the cleft on the structure of human CRP (1GNH, original X-ray crystallographic structure). (**D**) shows the cleft on the modelled modified structure in which the two fragments are missing. Colours denote the different parts of cleft in both the panels: deep pink and cyan are the two rims of the cleft; deep blue and light blue are the two sides of the cleft, in the floor towards the open end: cyan and light pink; two asparagine residues which are centrally located are coloured purple; beneath the cleft floor, the disulphide bridge is in gold and red (amino acids 1–6, QTDMSR) constitute the other side wall and yellow (amino acids 189–191, ALK) segments are the motifs that are absent in the modified variants of the CRP purified from patients.

sites lie on the opposite side of the pentraxin structure as shown in Figure 8(B). Hence the removal of these two segments would not directly affect the structure of the known functional motifs of the human CRP.

On the basis of the X-ray crystal structure of human CRP [2], the existence and importance of a cleft on the surface opposite to the Ca^{2+}- and PC-binding side was highlighted, but no known function could be assigned to it. However, more recently, the cleft is thought to be involved in C1q and FcR binding [26,27]. There are two potential N-glycosylation residues on the floor of the cleft, namely Asn^{158} and Asn^{160}. In the native structure (Figure 8C; coloured violet), the accessibility of these glycosylation sites is hindered by the presence of the N-terminal (amino acids 1–6; coloured red) and a portion of the rim of the cleft (amino acids 186–188; coloured deep blue). In the modified model (Figure 8D), these sites are fully exposed due to the removal of six N-terminal residues and sliding out of the C-terminal residues (amino acids 186–188; coloured deep blue) due to the removal of the ALK segment, thus facilitating glycosylation at these potential sites.

DISCUSSION

Increased levels of CRP correlate well with the extent of the inflammatory stimulus, tissue damage or trauma [28,29]. Monitoring its level is used to assess results of various treatment regimens [30]. The nature of non-specific elevation is an important obstacle for its wide clinical application, as it cannot be used for specific disease diagnosis. Despite extensive studies, no information is available regarding the existence of different molecular forms of human CRP with respect to carbohydrate moieties, amino-acid sequence or other chemical groups. It is difficult to compare differences between the normal and induced forms of human CRP because the basal level is very low. Therefore, to examine the molecular nature of different induced forms of CRP, we have used a number of clinical samples from six different pathological conditions. The major achievement of this investigation is the demonstration, for the first time, that human CRP is glycosylated.

Variations in electrophoretic mobilities (Figures 1A, 1B and 1D) gave us the first indication that distinct chemical entities might be induced in these six different pathological conditions. Our results strongly suggest that such variations at the molecular level occurred due to the variations both in carbohydrate (Tables 1–3) and amino-acid (Table 4) compositions. The presence of carbohydrates in CRPs is demonstrated by the results obtained using DIG glycan detection kits (Figures 3A and 3B), binding with ConA (Figures 5A–5C), SNA, MAA (Figure 3C) and other lectins (Table 3), an increase in pI after sialidase treatment (Figure 2, lane 8), reactivity towards N-glycosidase F (Figure 6) and, more conclusively, by analytical methods such as GLC and GLC–MS (Figures 4A–4C). Although the precise implication of this glycosylation is still an open question, glycosylation and variation in pI values may result in the specific binding to viruses, bacteria or other pathogens, and might possibly affect its biological activity through activation of the alternative complement pathway, agglutination, binding to lymphocytes, chromatin, histone and ribonucleoprotein particles.

Depending on the nature of pathological conditions, CRPs were induced to different levels of elevation (Table 1). The correlation of this elevation to the pattern of production of specific cytokines, their modulators and other extracellular signalling molecules is yet to be resolved. However, levels may be anticipated for combating the different clinical symptoms depending on the degree of damage *in vivo*. CRP, along with fibrinogen and interleukins, is reported to increase in high-risk coronary artery diseases, and its level could predict future risk. Based on an earlier observation that CRP increases the uptake of VL promastigotes into human macrophages, the capacity of equal amounts of three different glycosylated variants of CRP from VL, ALL and SLE to infect macrophages with *Leishmania donovani* was compared. The total number of macrophages infected with parasite was much higher in the presence of CRP (VL) as compared with ALL and SLE (T. Das and C. Mandal, unpublished work). Thus it may be envisaged that small variations in CRP structure may also have significant effects on their biological function.

The presence of glycosylation is demonstrated further by the decrease in molecular mass of approx. 2–4 kDa after removal of the sugar moiety (Figure 6). Considering the purification procedure, stringency of analyses, ConA-binding specificity, DIG detection after SDS/PAGE and Western blot, the presence of non-covalently bound sugars is highly unlikely.

Sialic acids are reported to have a major regulatory role in a multitude of cellular and molecular interactions [19,31–35]. A direct linkage in the degree of complement-mediated haemolysis with the presence of 9-O-acetylated sialic acid on human erythrocytes has been demonstrated [36]. Levels of sialic acids may represent acuteness of the disease and, accordingly, may be required to combat the various causative agents. The functional and structural diversity of CRP isolated from fish has been established on the basis of their carbohydrate-binding properties [9–12]. Therefore, sialic acids present in human CRP may be required to combat the various causative agents.

Slight differences in the pI (7.9–9) of CRPs (Figure 2) indicate their charge heterogeneity, which may arise owing to the net contribution of acidic amino acids and sialic acid sugars. Variations in pI of human CRP ranging from 5.4 to 7.9 has been reported [37,38], without paying much attention to the causes of such variations. It is more likely that these altered molecular variants of CRP are needed, as their main function is to bind and detoxify harmful substances that gain access to the circulation.

Sequence analysis of CRPs from three patients using MALDI showed the absence of two short segments: one from the N-terminus and another from the C-terminal end (Figure 7; Table 4). Molecular modelling of the modified CRP revealed that the structural motifs of all the known functions of CRP remained unaffected by such modification. However, the structure of the cleft on the surface opposite the Ca^{2+}- and PC-binding region was drastically altered so as to expose the potential glycosylation sites Asn^{158} or Asn^{160} on the cleft floor. Interestingly, the reduction in the molecular mass (Figure 6) suggests the glycosylation at the amide nitrogen (Figures 8A–8D).

It may be mentioned that the well-known N-glycosylation motif (Asn-Xaa-Ser/Thr, where Xaa is any amino acid other than proline) is not present in the amino-acid sequence of human CRP. The probable site, indicated by molecular modelling, contains the Asn-Val-Asn (amino acids 158–160) sequence, which is structurally very similar to the known motif. Significance of the existence of such a motif is the expression of some glycosyltransferase enzyme, which can act on the structural environment provided by that specific sequence of the motif only. This motif sequence of Asn-Val-Asn is structurally so similar to Asn-Val-Ser or Asn-Val-Thr that the same enzyme may catalyse it; however, the possibility of the expression of a currently undiscovered glycosyltransferase cannot be ruled out.

Our studies clearly demonstrate that CRPs induced in different pathological conditions differ both in their carbohydrate and amino-acid sequences. Observed differences in the electrophoretic mobility of the induced CRPs in the native gels may be the cumulative effects of small differences of the monomers in the resulting pentraxin structures. Small, but significant, differences in binding of ConA and other lectins, GLC and GLC–MS analysis, and pI may be attributed to their differences in amino-acid and carbohydrate contents. Differential lectin-like behaviour, sugar-binding properties and immunological reactivity of invertebrate [4] and human CRPs [39] also suggest differences in their structures and functions. Preferential glycosylation is possibly an altered post-translational modification, which may bear some relevance to the clearing of the inducing agents. Thus these differences in sequences may be explained without invoking the presence of different gene-induced splicing variations at post-transcriptional level. CRPs purified from pooled sera of five individuals with SLE showed a single band, suggesting identical variation. Similar results were also obtained with other diseases, indicating a similar type of variation. Alternatively, CRPs purified separately from the sera of several individuals suffering VL showed a single band with same mobility, providing proof of the induction of the similar CRP (Figure 1C).

The possibility of induction of some glycosyltransferases needed for post-translational enzyme regulation cannot be ruled out, as preferential expression of certain genes in the presence of toxic materials may facilitate the level of glycosylation differently during post-translational modification. In this context, it may be stated that the CRPs are modified differently, keeping their pentraxin structures almost the same as the native CRP, but some minor changes in their amino-acid sequence and glycosylation make them differ chemically, which may be essential for their proper biological function. These results may have far-reaching practical applications for monitoring the acute-phase responses.

In conclusion, it may be emphasized that our studies demonstrate convincingly the glycosylation of CRP, a finding that has never been reported in the case of humans, despite extensive studies on its induction in an enormous number of diseases. Our findings should stimulate an intensive search for such specific variants of human CRP of immense clinical importance, helpful for the diagnosis and monitoring of different clinical samples under a variety of pathological instances, which would open up a new avenue. These observations may pave the way for overcoming many important obstacles for the clinical use of CRP measurement and for new diagnostic approaches for using CRP as a potential clinical marker.

T. D. receives her senior research fellowship from the Council of Scientific and Industrial Research, New Delhi, India. We are thankful to Dr M. Chatterjee for helpful discussion and Mr A. Mallick for his excellent technical help.

REFERENCES

1 Pepys, M. B. (1981) C-reactive protein fifty years on. Lancet **i**, 653–657
2 Shrive, A. K., Cheetham, G. M. T., Holden, D., Myles, D. A. A., Turnell, W. G., Volanakis, J. E., Pepys, M. B., Bloomer, A. C. and Greenhough, T. J. (1996) Three dimensional structure of human C-reactive protein. Nat. Struct. Biol. **3**, 346–354
3 Volanakis, J. E. (2001) Human C-reactive protein: expression, structure, and function. Mol. Immunol. **38**, 189–197
4 Mandal, C., Biswas, M., Nagpurkar, A. and Mookerjea, S. (1991) Isolation of a phosphoryl choline-binding protein from the hemolymph of the snail, *Achatina fulica*. Dev. Comp. Immunol. **15**, 227–239
5 Mandal, C., Sinha, S. and Mandal, C. (1999) Lectin like properties and differential sugar binding characteristics of C-reactive proteins purified from sera of normal and pollutant induced *Labeo rohita*. Glycoconj. J. **16**, 741–750
6 Gabay, C. and Kushner, I. (1999) Acute phase proteins and other systemic responses to inflammation. N. Engl. J. Med. **340**, 448–454
7 Weinhold, B. and Ruther, U. (1997) Interleukin-6-dependent and -independent regulation of the human C-reactive protein gene. Biochem. J. **327**, 425–429
8 Weinhold, B., Bader, A., Poli, V. and Ruther, U. (1997) Interleukin-6 is necessary, but not sufficient, for induction of the human C-reactive protein gene *in vivo*. Biochem. J. **325**, 617–621
9 Sinha, S. and Mandal, C. (1996) Microheterogeneity of C-reactive protein in the sera of fish *Labeo rohita* induced by metal pollutants. Biochem. Biophys. Res. Commun. **226**, 681–687
10 Sinha, S., Mandal, C. N., Allen, A. K. and Mandal, C. (2001) Acute phase response of C-reactive protein of *Labeo rohita* to aquatic pollutants is accompanied by the appearance of distinct molecular forms. Arch. Biochem. Biophys. **369**, 139–150
11 Paul, I., Mandal C. and Mandal, C. (1998) Effect of environmental pollutants on the C-reactive protein of a freshwater major carp, *Catla catla*. Dev. Comp. Immunol. **22**, 519–532
12 Paul, I., Mandal, C., Allen A. K. and Mandal. C. (2001) Molecular variants of C-reactive proteins from the major carp *Catla catla* in fresh and polluted aquatic environments. Glycoconj. J. **18**, 547–556
13 Volanakis, J. E., Clements, W. L. and Schrohenloher, R. E. (1978) C-reactive protein: purification by affinity chromatography and physiochemical characterization. J. Immunol. Methods **23**, 285–295
14 Davis, B. J. (1964) Disc electrophoresis II. Method and application to human serum proteins. Ann. N.Y. Acad. Sci. **121**, 404–427
15 Laemmli, U. K. and Favre, M. (1973) Maturation of head of bacteriophage T4. I. DNA packaging events. J. Mol. Biol. **80**, 575–599
16 O'Farrell, P. Z., Goodman, H. M. and O'Farrell, P. H. (1977) High resolution two-dimensional electrophoresis of basic as well as acidic proteins. Cell, **12**, 1133–1141
17 Sharma, V., Chatterjee, M., Mandal, C., Basu, D. and Sen, S. (1998) Rapid diagnosis of visceral leishmaniasis using Achatinin-H, a 9-O-acetylated sialic acid binding lectin. Am. J. Trop. Med. Hyg. **58**, 551–554
18 Sloneker, J. H. (1972) Gas–liquid chromatography of alditol acetates. In Methods in Carbohydrate Chemistry (R. L. Whistler and J. N. BeMiller, eds.), vol. VI, pp. 20–24, Academic Press, New York
19 Lönngren, J. and Svensson, S. (1974) Mass spectrometry in structural analysis of natural carbohydrates. Adv. Carbohydr. Chem. Biochem. **29**, 41–106

20 Hunter, W. M. (1978) in: Handbook of Experimental Immunology (Weir, D. M., ed.) pp. 14.1–14.3, Blackwell Scientific, London
21 Scatchard, G. (1949) The attractions of proteins for small molecules and ions. Ann. N.Y. Acad. Sci. **51**, 660–672
22 Mandal, C., Basu, S. and Mandal C. (1989). Physicochemical studies on achatininH, a novel sialic acid-binding lectin. Biochem. J. **257**, 65–71
23 Kuhn, J., Gotting, C., Schnolzer, M., Kempf, T., Brinkmann, T. and Kleesiek, K. (2001) First isolation of human UDP-D-xylose: proteoglycan core protein β-D-xylosyltransferases secreted from cultured JAR choriocarcinoma cells. J. Biol. Chem. **276**, 4940–4947
24 Mandal, C., Kingery, B.D., Anchin, J.M., Subramanium, S. and Linthicum. D. S. (1996). ABGEN: a knowledge-based automated approach for antibody structure modeling. Nat. Biotechnol. **14**, 323–328
25 Reference deleted
26 Agrawal, A., Shrive, A. K., Greenhough, T. J. and Volanakis, J. E. (2001) Topology and structure of the C1q-binding site on C-reactive protein. J. Immunol. **166**, 3998–4004
27 Marnell, L. L., Mold, C., Volzer, M. A., Burlingame, R. W. and Du Clos, T. W. (1995) C-reactive protein binds to FcγRI in transfected COS cells. J. Immunol. **155**, 2185–2193
28 Taskinen, S., Kovanen, P. T., Jarva, H., Meri, S. and Pentikainen, M. O. (2002) Binding of C-reactive protein to modified low-density-lipoprotein particles: identification of cholesterol as a novel ligand for C-reactive protein. Biochem. J. **367**, 403–412
29 Fu, T. and Borensztajn, J. (2002) Macrophage uptake of low-density lipoprotein bound to aggregated C-reactive protein: possible mechanism of foam-cell formation in atherosclerotic lesions. Biochem. J. **366**, 195–201
30 Albert, C. M., Ma, J, Rifai, N, Stampfer, M. J. and Ridker P. M. (2002) Prospective study of C-reactive protein, homocysteine, and plasma lipid levels as predictors of sudden cardiac death. Circulation **105**, 2595–2599
31 Mandal, C., Chatterjee, M. and Sinha, D. (2000) Investigation of 9-O-acetylated sialoglycoconjugates in childhood acute lymphoblastic leukaemia. Br. J. Haematol. **110**, 801–812
32 Sinha, D., Chatterjee, M. and Mandal, C. (2000) O-acetylation of sialic acids – their detection, biological significance and alteration in diseases. Trends Glycosci. Glycotechnol. **12**, 17–33
33 Pal, S., Chatterjee, M., Bhattacharya, D. K., Bandhyopadhyay, S. and Mandal, C. (2000) Identification and purification of cytolytic antibodies directed against O-acetylated sialic acid in childhood acute lymphoblastic leukemia. Glycobiology **10**, 539–549
34 Sinha, D., Mandal, C. and Bhattacharya. D. K. (1999) Identification of 9-O acetyl sialoglycoconjugates (9-OAcSGs) as biomarkers in childhood acute lymphoblastic leukemia using a lectin, AchatininH, as a probe. Leukemia **13**, 119–125
35 Chatterjee, M., Sharma, V., Sundar, S., Sen, S. and Mandal, C. (1998) Identification of antibodies directed against O-acetylated sialic acids in visceral leishmaniasis: its diagnostic and prognostic role. Glycoconj. J. **15**, 1141–1147
36 Sharma, V., Chatterjee, M., Sen, G., Chava A. K. and Mandal, C. (2000) Role of linkage specific 9-O-acetylated sialoglycoconjugates in activation of the alternate complement pathway on mammalian erythrocytes. Glycoconj. J. **17**, 887–893
37 Baltz, M. L., De Beer, F. C., Feinstein, A., Munn, E. A., Fletcher, T. C., Taylor, J., Bruton, C., Clamp, J. R., Davies, A. J. S. and Pepys, M. B. (1982) Phylogenetic aspects of C-reactive protein and related protein. Ann. N.Y. Acad. Sci. **389**, 49–75
38 Lasson, A. and Goransson, J. (1999) No microheterogenous changes of plasma C-reactive protein found in man during various diseases. Scand. J. Clin. Lab. Invest. **59**, 293–304
39 Kottgen, E., Hell, B., Kage, A. and Tauber, R. (1992) Lectin specificity and binding characteristics of human C-reactive protein. J. Immunol. **149**, 445–453

Received 31 October 2002/26 February 2003; accepted 14 April 2003
Published as BJ Immediate Publication 14 April 2003, DOI 10.1042/BJ20021701